PERFORMANCE ANALYSIS OF GRAY LEVEL CO-OCCURRENCE MATRIX TEXTURE FEATURES FOR GLAUCOMA DIAGNOSIS

[1]Sakthivel Karthikeyan and [2]N. Rengarajan

[1]Department of ECE, K.S.R. College of Engineering, Tiruchengode, India
[2]K.S.R. College of Engineering, Tiruchengode, TamilNadu, India

ABSTRACT

Glaucoma is a multifactorial optic neuropathy disease characterized by elevated Intra Ocular Pressure (IOP). As the visual loss caused by the disease is irreversible, early detection is essential. Fundus images are used as input and it is preprocessed using histogram equalization. First order features from histogram and second order features from Gray Level Co-occurrence Matrix (GLCM) are extracted from the preprocessed image as textural features reflects physiological changes in the fundus images. Second order textural features are extracted for different quantization levels namely 8, 16, 32, 64, 128 and 256 in four orientations viz 0, 45, 90 and 135° for various distances. Extracted features are selected using Sequential Forward Floating Selection (SFFS) technique.The selected features are fed to Back Propagation Network (BPN) for classification as normal and abnormal images. The proposed computer aided diagnostic system achieved 96% sensitivity, 94% specificity, 95% accuracy and can be used for screening purposes. In this study, the analysis of gray levels have shown their significance in the classification of glaucoma.

Keywords: Glaucoma, GLCM, Texture, Quantization Level, Back Propagation

1. INTRODUCTION

Glaucoma, the second leading cause of blindness is characterized by the progressive degeneration of optic nerve fibers, the "cable" that transmits the visual message from the eye to the brain and characteristic damage to the visual field. A survey shows that the glaucoma is responsible for 6 million cases worldwide. The main risk factor of glaucoma is elevated pressure in the eye which causes damage to the eye optic nerve. It also affects the optic disc by enlarging the cup size. It is possible that early functional changes are detectable before significant loss occurs, at a stage where they may still be reversible through early intervention.

As last capabilities of the optic nerve cannot be recovered, early diagnosis is important to stop or slow down disease progression. Presently, state-of-the art glaucoma detection requires mass screening. A glaucoma diagnosis system based on texture features using the less expensive digital fundus images are analyzed to discriminate normal and glaucomatous images.

Glaucoma Risk Index (GRI) was described by Bock *et al*. (2010) to assess glaucoma. The accuracy of 80% has been achieved in a 5-fold cross-validation setup and the GRI gains an Area Under Convergence (AUC) of 88%. Tan *et al*. (2010) analyzed ocular thermal images with second-order texture features together with first-order texture analysis, moments and difference histogram. Several significant linear correlations among investigated features were observed. The features extracted from cross co-occurrence matrix played an important role in the diagnosis of ocular diseases.

Texture provides important information about the structural arrangement of surfaces and their relationship to the surrounding environment. The textural properties of images appear to carry useful information for discrimination purposes and hence texture analysis of fundus image is performed. Ramamurthy and Chandran (2012) developed


Corresponding Author: Sakthivel Karthikeyan, Department of ECE, K.S.R. College of Engineering, Tiruchengode, India

an efficient image retrieval systems using Gray Level Co-occurrence Matrix statistical measures computed provide increasing similarities between query image and database images for improving the retrieval performance along with the large scalability of the databases. Veluchamy *et al.* (2012) segmented blood cells using morphological operations and extracted first, second order gray level statistics and geometrical parameters. Features extracted achieved 80% classification accuracy.

Kavitha and Duraiswamy (2011) used texture features to discriminate between normal and nonproliferative eyes from the quantitative assessment of monocular fundus images. Two parameters energy and contrast were considered to be the most efficient for discriminating different textural patterns. A novel glaucoma detection system using a combination of texture and higher order spectra features proposed by Rajendra *et al.* (2011) provided an accuracy of more than 91%. Yogesh and Sasikala (2012) described texture analysis of retinal layers in spectral domain OCT in which diagnosis of age related macular degeneration, diabetic macular edema was tested. The behavior of co-occurrence statistics was investigated by Gomez *et al.* (2012) to classify Breast Ultrasound (BUS) images. The best AUC of 0.81 was achieved with 32 gray levels and 109 features. AUC of 0.87 was obtained for single texture feature. The texture descriptors that contributed notably to distinguish lesions were contrast and correlation.

Krishnan and Oliver (2013) proposed an automated glaucoma diagnosis system based on hybrid feature extraction from digital fundus images. Further a novel integrated index called Glaucoma Risk Index (GRI) which is composed from HOS, TT and DWT features, is used to diagnose the unknown class using a single feature during the mass screening of normal/glaucoma images. Most of the shape based approaches assume a valid segmentation of the optic disk. However, a small error in these segmentation based techniques may result in significant changes in the measurements and leads to errors in the diagnosis. As feature extraction is performed in the digital domain, the proposed glaucoma diagnosis system can be easily incorporated into existing medical image analysis for large scale screening. So a glaucoma diagnosis system is proposed based on the analysis of gray levels in different orientations using digital fundus images (**Fig. 1**). Nyul (2009) focused on a novel automated classification system for glaucoma, based on image features from fundus photographs. Extracted high-dimensional feature vectors are compressed via Principal Component Analysis (PCA) and combined with Support Vector Machine (SVM). In this technique, accuracy of detecting glaucomatous retina fundus images are comparable to that of human experts.
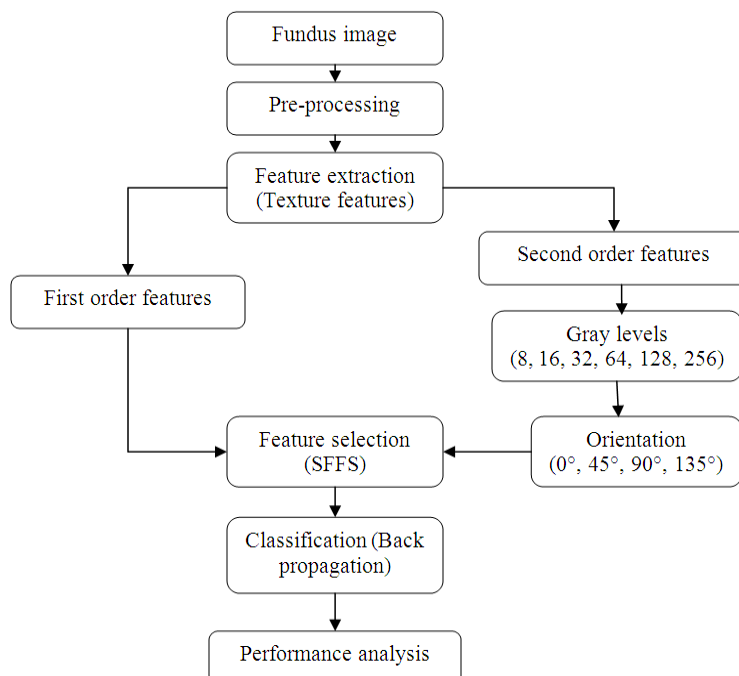
Fig. 1. Proposed method to detect glaucoma

Texture features are chosen since fundus images reflect the physiological changes that occur due to glaucoma progression. Glaucoma diagnosis system is proposed in this study based on the behavior of texture features as a function of gray-level quantization to classify retinal images. Different gray levels are analyzed to clearly discriminate between the normal and abnormal stages.

2. MATERIALS AND METHODS

After preprocessing, the acquired fundus images, texture based features are extracted for different quantization levels and subjected to feature selection process. Subsequently, these features are fed to back propagation network for classification. Further an analysis on the influence of different features is performed to assess glaucoma.

2.1. Data

Fundus images are captured by Topcon TRC50 EX mydriatic fundus camera with a 50° field of view at Aravind eye hospital, Madurai. The image size is 1900×1600 pixels at 24 bits true color image. Doctors in the ophthalmic department of the hospital approved the images for the research purpose. Various stages of glaucoma affected fundus images are taken from http://www.optic-disc.org, a public database.

2.2. Preprocessing

The retinal images are pre-processed to improve the local contrast of an image and bring out more detail.

Image contrast is enhanced using histogram equalization by transforming the values in an intensity image. **Figure 2** describes the histogram equalized image.

2.3. Texture Features

Texture analysis refers to the description of characteristic image properties by textural features. Texture is a result of local variations in brightness within one small region of an image. Naseri *et al.* (2012) described texture as a measure of surface roughness when the intensity values of an image are considered to be elevations.

Four first order features namely Mean, Standard deviation, Entropy and Variance are extracted from the preprocessed image. Second order textural features are then extracted using Gray-Level Co-occurrence Matrix (GLCM) to represent a set of features to reduce the misclassification of glaucomatous images. GLCM depicts how different combinations of pixel brightness values occur in an image.It is a second-order measure because it measures the relationship between neighboring pixels. GLCM represents the joint frequencies of all pair wise combinations of gray levels i and j separated by a distance along a direction θ as shown in Equation (1). Then, the GLCM can be defined as:

$$C(i,j) = \| \langle \{[(x_1,y_1),(x_2,y_2)]\} | x_2, y_2 | d \cos \theta$$
$$y_2 - y_1 = d \sin \theta, I(x_1,y_1) = i, I(x_2, y_2) = j \| \tag{1}$$
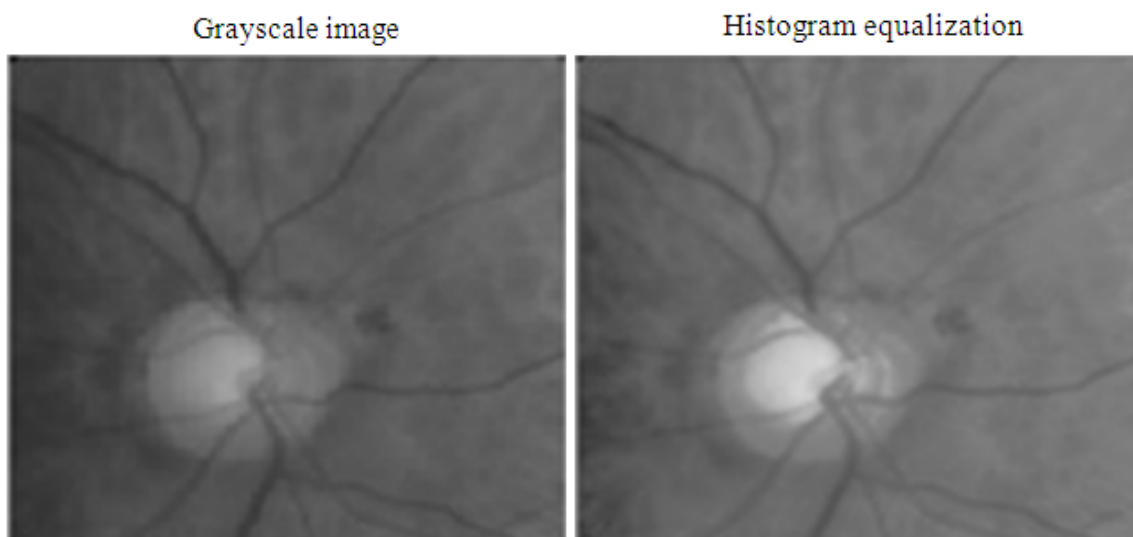
Fig. 2. Grayscale fundus image and histogram equalized image

Where:

(x_1, y_1) and (x_2, y_2) = Pixels in the Region Of Interest (ROI)

$I(\cdot)$ = The gray-level of the pixel

$\|\cdot\|$ = The number of the pixel pairs that satisfy the conditions

Each GLCM was normalized by the sum of all its elements to calculate the co-occurrence relative frequency between gray level i and j. Each entry in GLCM matrix is considered to be the probability that a pixel with value i will be found adjacent to a pixel of value j as in Equation (2):

$$G = \begin{bmatrix} p(1,1) & p(1,2) & \cdots & p(1,Ng) \\ p(2,1) & p(2,2) & \cdots & p(2,Ng) \\ \vdots & \vdots & & \vdots \\ p(Ng,1) & p(Ng,2) & \cdots & p(Ng,Ng) \end{bmatrix} \quad (2)$$

Twenty two features were extracted from the GLCM matrix viz. autocorrelation, contrast, correlation I, correlation II, cluster prominence, cluster shade, dissimilarity, energy, entropy, homogeneity I, homogeneity II, maximum probability, sum of squares, sum average, sum entropy, sum variance, difference variance, difference entropy, information measure of correlation I, information measure of correlation II, inverse difference normalized and inverse difference moment normalized are extracted from the GLCM matrix. The process is continued for six quantization levels (8, 16, 32, 64, 128 and 256) for orientations of 0, 45, 90 and 135° in various distances d = 1,2,3,4. Thus twenty four co-occurrence matrices were obtained for graylevels in different orientations.

2.4. Feature Selection

High dimension data could contain high degree of redundant information and degrade the efficiency of the system. Hence feature selection process is performed using Sequential Floating Forward Selection (SFFS) feature selection method. This method is used to deal with the nesting problem. The best subset of features was initialized as the empty set and at each step a new feature was added. After that, the algorithm searches for features that can be removed until the correct classification error does not increase. The "best subset" of features is constructed based on the frequency with which each attribute is selected. The selected features are provided as input for the classification.

2.5. Classification

Back propagation is a common method of training artificial neural networks. The network learns from many inputs, to get the desired output. It is a supervised learning method and is a generalization of the delta rule. It requires a dataset of the desired output for many inputs, making up the training set. It is most useful for feed-forward networks (networks that have no feedback, or simply, that have no connections that loop). Helmy and El-Taweel (2010) developed a neural network model for satellite images based on both spectral and textural analysis. Better discrimination with 23% higher accuracy was achieved in the trained network with textural features than without textural parameters.

2.6. Performance Analysis of Textural Features

Discrimination of normal and abnormal images for different textural features are analyzed using box-plot. The box-plot for three features namely contrast, entropy and cluster prominence in four orientations 0, 45, 90 and 135° are shown from **Fig. 3-5**.

From the GLCM matrix, second order features were extracted in different orientations for gray levels of 8, 16, 32, 64, 128. Feature values derived for gray levels 8 and 16 are shown in **Table 1 and 2** has the feature values derived for gray level 32 and 64 for an orientation of 0°.

Table 1. Gray level analysis (8 and 16) at an orientation of 0°

Features	Normal image (Gray level 8)	Abnormal image	Normal image Gray level 16	Abnormal image
Autocorrelation	19.6724±0.6426	25.1933±4.7872	70.2527±2.5996	62.8439±19.65
Contrast	0.1966±0.0369	0.3208±0.0532	0.5232±0.1347	1.0604±0.2063
Cluster Prominence	27.6587±7.3438	50.5154±29.2446	500.51±134.80	997.67±579.14
Cluster shade	1.7675±0.4431	-1.3265±2.8259	15.8089±4.8111	-11.8421±27.88
Dissimilarity	0.1887±0.0300	0.2552±0.0343	0.3945±0.0686	0.5523±0.0729
Entropy	1.7924±0.1443	2.1351±0.2289	2.8897±0.1983	3.3279±0.2720
Homogeneity I	0.9069±0.0139	0.8810±0.0152	0.8209±0.0264	0.7733±0.252
Maximum probability	0.3764±0.0375	0.3053±0.0704	0.1835±0.0457	0.1183±0.0320
Sum of squares	19.6341±0.6641	25.1782±4.8057	70.4552±2.6776	93.2052±19.78
Sum entropy	52.9257±2.6862	67.2203±12.9962	16.4438±0.3431	18.7151±2.0984

**Table 2.** Gray level analysis (32 and 64) at an orientation of 0°

Features	Normal Image (Gray level 32)	Abnormal image	Normal Image Gray level 64	Abnormal image
Autocorrelation	265.0913±10.2628	356.3814±79.3501	1028.9513±41.3399	1395.8359±318.6941
Contrast	1.7708±0.5585	3.9982±0.8582	6.8167±2.2880	15.9458±3.5025
Cluster prominence	8991.2103±2432.8	17918.7635±10473.9	152593.7908±41032.	303960.5089±178195
Cluster shade	139.5198±41.49	-106.4772±246.42	1186.6093±347.25	-902.5100±2057.95
Dissimilarity	0.8140±0.1440	1.1379±0.1511	1.6562±0.2917	2.3091±0.3033
Entropy	4.1395±0.2315	4.6067±0.2947	5.4648±0.2476	5.9386±0.2996
Homogeneity I	0.6950±0.0370	0.6310±0.0318	0.5461±0.0402	0.4781±0.0305
Maximum probability	0.0699±0.0207	0.0432±0.0137	0.0219±0.0073	0.0117±0.0029
Sum of squares	265.8720±10.72	357.9485±79.85	1032.2587±42.86	1402.1924±320.76
Sum entropy	864.2195±38.7961	1183.5579±278.3042	3638.2343±158.2517	5004.3127±1184.2843

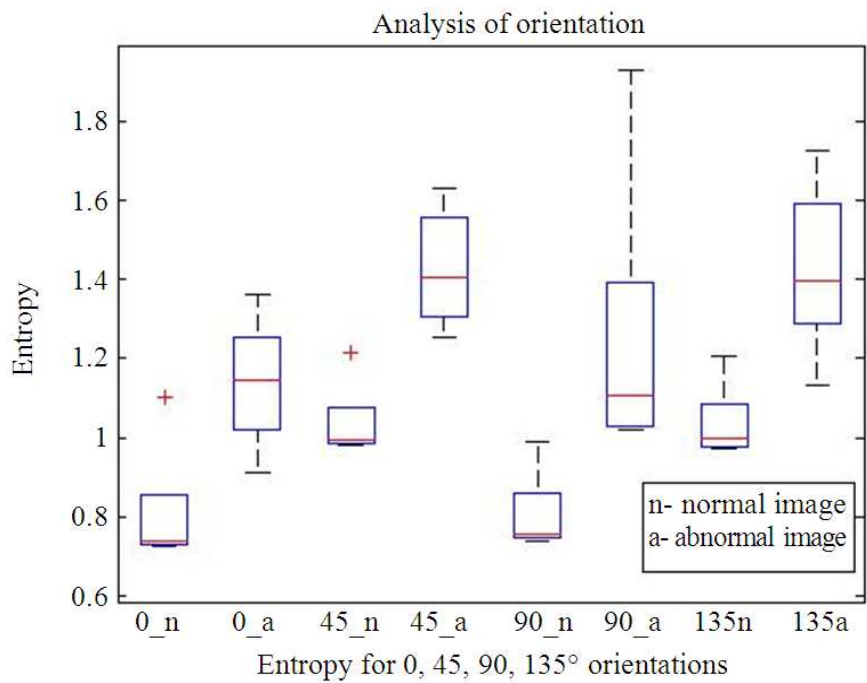**Table 3.** Analysis of gray level 32 in orientations (0°, 45°)

Features	Normal Image Orientation (0°)	Abnormal Image	Normal Image Orientation (45°)	Abnormal image
Autocorrelation	0265.0913±10.2628	356.3814±79.3501	264.4592±10.4221	355.9416±79.3203
Contrast	1.7708±0.5585	3.9982±0.8582	2.9479±0.8615	5.2020±1.1928
Correlation I	0.9260±0.0113	0.8951±0.0141	0.8763±0.0181	0.8641±0.0180
Correlation II	0.9260±0.0113	0.8951±0.0141	0.8763±0.0181	0.8641±0.0180
Cluster prominence	8991.210±2432.8386	17918.76±10473.92	8722.1606±2367.19	17490.01±10359.83
Cluster shade	139.5198±41.4956	-106.477±246.4245	143.0857±42.9206	-100.8091±249.535
Dissimilarity	0.8140±0.1440	1.1379±0.1511	1.0805±0.1670	1.3879±0.1834
Energy	0.0279±0.0071	0.0163±0.0051	0.0222±0.0055	0.0135±0.0044
Entropy	4.1395±0.2315	4.6067±0.2947	4.3627±0.2237	4.7941±0.3002
Homogeneity I	0.6950±0.0370	0.6310±0.0318	0.6336±0.0332	0.5812±0.0316
Homogeneity II	0.6736±0.0425	0.6010±0.0383	0.6029±0.0396	0.4501±0.2149
Maximum probability	0.0699±0.0207	0.0432±0.0137	0.0579±0.0178	89.8751±179.6725
Sum of squares	265.8720±10.7234	357.9485±79.8564	265.9770±10.7624	276.2963±134.6501
Sum average	31.8670±0.6937	36.5420±4.3358	31.8702±0.6947	328.5704±586.3273
Sum entropy	864.2195±38.7961	1183.5579±278.304	863.3759±39.2780	863.3759±39.2780
Sum variance	3.2690±0.1110	3.5168±0.1787	3.2632±0.1088	4.0240±1.1273
Difference variance	1.7708±0.5585	3.9982±0.8582	2.9479±0.8615	4.2823±1.6929
Difference entropy	1.1898±0.0966	1.3855±0.1007	1.3712±0.0974	1.5348±0.1045
Information measure of correlation I	-0.4144±0.0316	-0.3853±0.0172	-0.3282±0.0260	-0.3196±0.0124
Information measure of correlation II	0.9401±0.0087	0.9423±0.0082	0.9045±0.0124	0.9152±0.0105
Inverse difference normalized	0.9762±0.0041	0.9676±0.0041	0.9687±0.0045	0.9608±0.0049
Inverse difference moment normalized	0.9983±0.0006	0.9963±0.0007	0.9972±0.0008	0.9952±0.0010

Feature values for gray level 32 analyzed for normal and abnormal images in orientations (0°, 45°) are shown in **Table 3** and orientations (90°, 135°) are shown in **Table 4**.
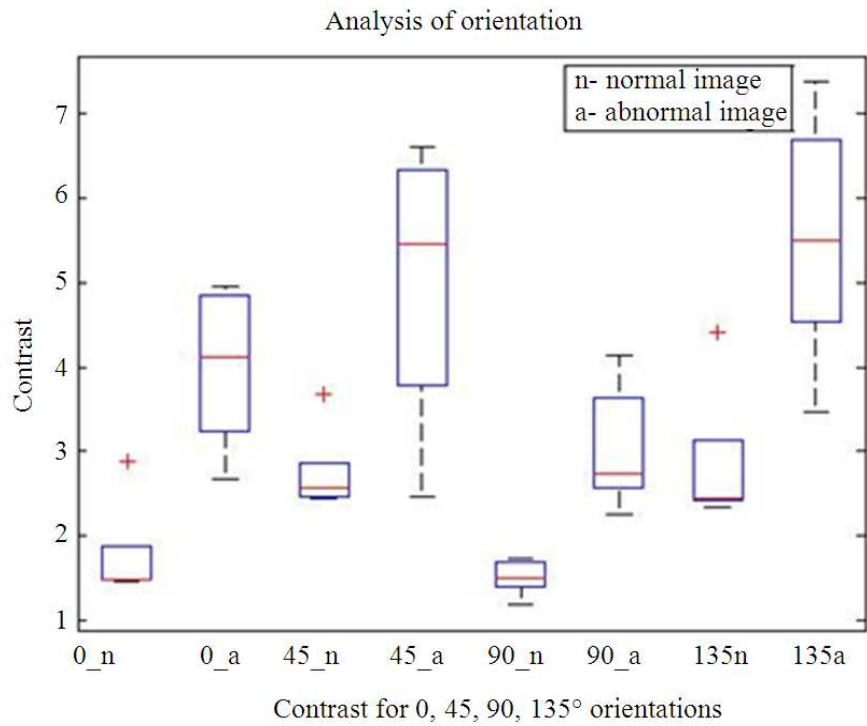
Fig. 3. Box-plot for contrast feature

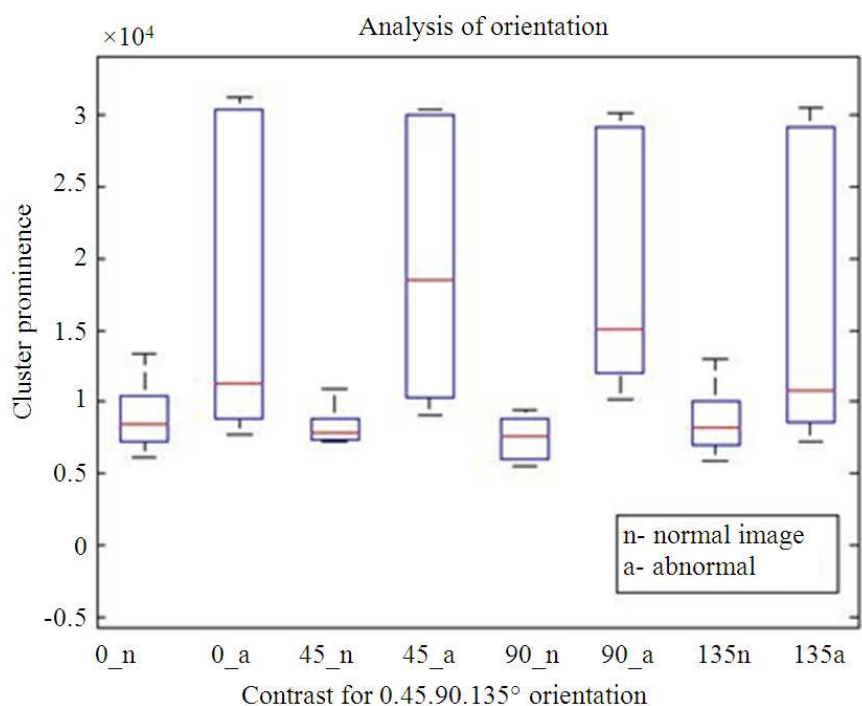**Fig. 4.** Box-plot for entropy feature

Fig. 5. Box-plot for cluster prominence feature

Table 4. Analysis of gray level 32 in orientations (90°, 135°)

Features	Normal image Orientation (90°)	Abnormal image	Normal image Orientation (135°)	Abnormal image
Autocorrelation	264.5648±10.4462	359.3770±79.7244	264.4956±10.4546	355.7721±79.2008
Contrast	1.7726±0.4807	2.0585±0.5111	2.8694±0.7790	5.5381±1.3334
Correlation I	0.9258±0.0085	0.9473±0.0064	0.8797±0.0129	0.8559±0.0175
Correlation II	0.9258±0.0085	0.9473±0.0064	0.8797±0.0129	0.8559±0.0175
Cluster prominence	9070.1472±2486.4366	19355.79±11155.29	8729.2809±2367.12	17240.02±10112.92
Cluster shade	137.4091±41.5344	106.63±260.1905	142.3549±42.6195	102.0237±235.863
Dissimilarity	0.8291±0.1318	0.9193±0.1343	1.0797±0.1649	1.4279±0.2001
Energy	0.0271±0.0067	0.0177±0.0056	0.0220±0.0056	0.0132±0.0043
Entropy	4.1594±0.2227	4.4923±0.2951	4.3675±0.2276	4.8153±0.3063
Homogeneity I	0.6890±0.0340	0.6611±0.0322	0.6329±0.0335	0.5768±0.0322
Homogeneity II	0.6669±0.0392	0.6357±0.0381	0.6015±0.0398	0.5360±0.0395
Maximum probability	0.0678±0.0202	0.0453±0.0153	0.0573±0.0179	0.0355±0.0116
Sum of squares	265.5272±10.4035	360.1860±79.9200	265.8475±10.4128	358.7191±79.6841
Sum average	31.8444±0.6837	36.6383±4.3366	31.8702±0.6947	36.5492±4.3400
Sum entropy	862.2998±39.1759	1191.7382±279.453	863.3780±39.2943	1183.15±278.1978
Sum variance	3.2716±0.1116	3.5351±0.1762	3.2644±0.1086	3.5086±0.1797
Difference variance	1.7726±0.4807	2.0584±0.5111	2.8694±0.7790	5.5381±1.3334
Difference entropy	1.1992±0.0895	1.2527±0.1006	1.3736±0.0976	1.5566±0.1119
Information measure of correlation I	0.4080±0.0269	0.4302±0.0138	0.3264±0.0250	-0.3123±0.0159
Information measure of correlation II	0.9381±0.0075	0.9559±0.0052	0.9036±0.0112	0.9113±0.0114
Inverse difference normalized	0.9757±0.0037	0.9730±0.0038	0.9687±0.0045	0.9598±0.0052
Inverse difference moment normalized	0.9983±0.0006	0.9980±0.0005	0.9973±0.0008	0.9949±0.0012

3. RESULTS

Performance of the classifier are measured in terms of sensitivity, specificity and accuracy. Sensitivity is a measure that determines the probability of results that are true positive such that the person is affected by the disease. Specificity is a measure that determines the true negatives such that the person is not affected by retinal disease. Accuracy is a measure that determines the results that are accurately classified. MATLAB version 7.12 is used for implementation of the work. Comparative analysis for all gray level quantization namely 8, 16, 32, 64, 128 and 256 are performed based on correctly classified images.

Impact of individual gray levels on the detection of normal and abnormal fundus image are given in **Table 5**. Graph showing the performance evaluation of various gray level quantization are shown in **Fig. 6**.

3.1. Training Performance Using BPN

The back propagation neural network was used for the classification of the fundus images. Classification is performed for all gray level quantization to determine the best discriminating gray level and the result shows that the gray level 32 classifies with higher accuracy. In this study, 50 images are used for training and 100 images for testing. About 50 images (25 normal and 25 abnormal) for training and 100 images (50 normal and 50 abnormal) for testing were used for classification. From the available dataset, data is split into set1 and testing set. Next, set1 is further divided into training and validation set. Then the classifier is trained using training set and tested on validation set. The process is repeated by selecting various combinations of training and validation set. The classifier which gives best performance is then selected and used to get performance in the testing set. The sample neural network results containing Receiver Operating Characteristic (ROC) curve plotted against false positive and true positive rate are shown in **Fig. 7**.

Table 5. Performance analysis of gray level

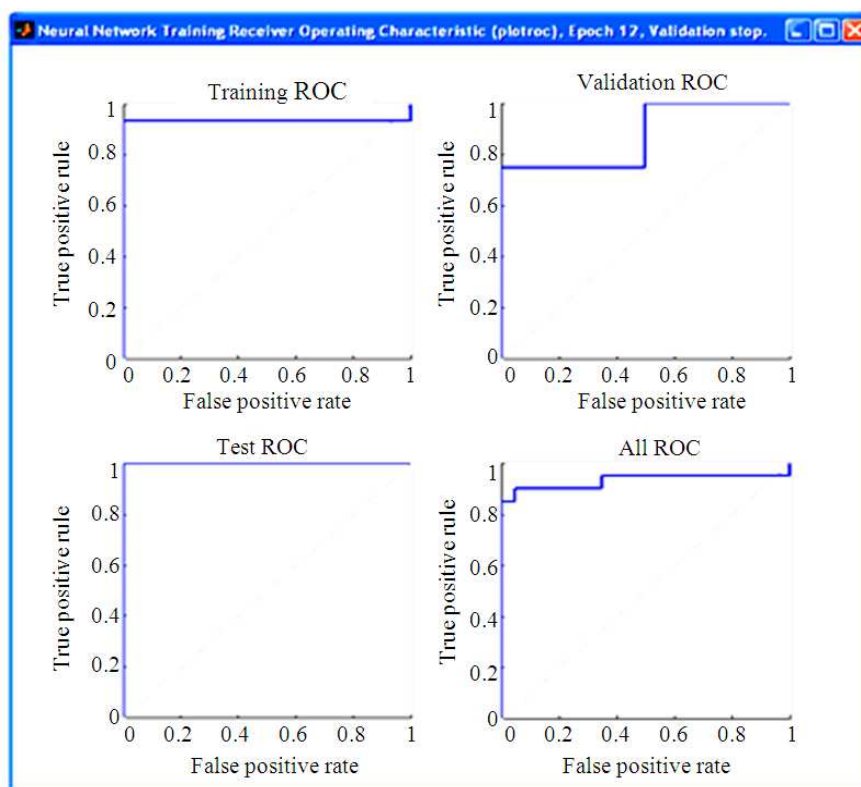| Gray level	Specificity (%)	Sensitivity (%)	Accuracy (%)
8	86	88	87
16	90	88	89
32	94	96	95
64	90	92	91
128	92	90	91
256	88	90	89
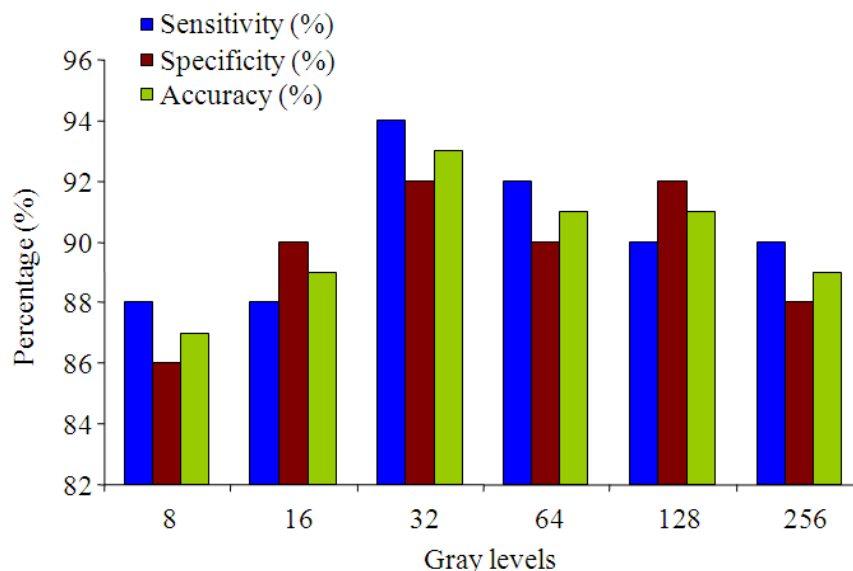
Fig. 6. Analysis of gray levels

Fig. 7. Performance analysis of classifier

4. DISCUSSION

Quantitative texture analysis was performed to improve diagnosis of retinal images. Features derived from the 32 gray levels classified 47 normal images correctly out of 50 normal images and 48 abnormal images as abnormal out of 50 abnormal images with an accuracy of 95%. The accuracies obtained for gray levels 8 and 16 were 87% and 89% respectively. For the gray level 256, the accuracy was about 89% and the computation complexity also increases. The gray levels 16 and 128 produced accuracy of 89% and 91% respectively, but its specificity was greater than the sensitivity. It means that the abnormal images were classified as normal which was undesirable. The gray level 32 classified the fundus images with specificity of 94%, sensitivity of 96% and accuracy of 95%. Thus gray level 32 holds good for the classification of the fundus images. First order feature viz. skewness and second order features contrast, correlation, dissimilarity, cluster prominence and autocorrelation showed good discrimination of normal and abnormal retinal images at 90° orientation for unit distance.

5. CONCLUSION

This study presented a study of co-occurrence texture statistics as a function of gray-level quantization for glaucoma diagnosis. The retinal images were preprocessed for improving the local contrast of an image and bringing out more detail. Twenty-two texture features autocorrelation, contrast, correlation I, correlation II, cluster prominence, cluster shade, dissimilarity, energy, entropy, homogeneity I, homogeneity II, maximum probability, sum of squares, sum average, sum entropy, sum variance, difference variance, difference entropy, information measure of correlation I, information measure of correlation II, inverse difference normalized and inverse difference moment normalized extracted from the GLCMs were extracted for different quantization levels 8, 16, 32, 64, 128 and 256 for 0, 45, 90 and 135° orientations for unit distance. Sequential Forward Floating Selection (SFFS) was used for feature selection. The selected features were fed as input to back propagation network to classify

the images as normal and abnormal. Features computed from GLCM with orientation of 90°, quantization level 32, unit distance contributed notably to distinguish between normal and abnormal fundus images. The proposed computer aided diagnostic system achieved 96% sensitivity, 94% specificity, 95% accuracy and can be used for screening purposes.

When more number of gray levels is included in GLCM, computational cost of texture statistics becomes higher. GLCM statistics can be used to discriminate between normal and abnormal images but GLCM texture features performs poorer in differentiating stages of abnormalities. Too many texture features affects classification rate and hence feature selection or significant tests are highly essential to identify selective features.

An efficient automatic system can be developed by including diverse images for the mass screening of glaucoma. Classification accuracy can be improved by increasing the number of training images and choosing better features. To identify disease progression, GLCM statistics can be combined with other texture features or geometrical features.

6. REFERENCES

Bock, R., J. Meier, L.G. Nyul, J. Honegger and G. Michelson, 2010. Glaucoma risk index: Automated glaucoma detection from color fundus images. Med. Image Anal., 14: 471-481. DOI: 10.1016/j.media.2009.12.006

Gomez, W., W.C.A. Pereira and A.F.C. Infantosi, 2012. Analysis of co-occurrence texture statistics as a function of gray-level quantization for classifying breast ultrasound. IEEE Trans. Med. Imag., 31: 1889-1899. DOI: 10.1109/TMI.2012.2206398

Helmy, A.K. and G.S. El-Taweel, 2010. Neural network change detection model for satellite images using textural and spectral characteristics. Am. J. Eng. Applied Sci., 3: 604-610. DOI: 10.3844/ajeassp.2010.604.610

Kavitha, S. and K. Duraiswamy, 2011. Adaptive neuro fuzzy inference system approach for the automatic screening of diabetic retinopathy in fundus images. J. Comput. Sci., 7: 1020-1026. DOI: 10.3844/jcssp.2011.1020.1026

Krishnan, M.M.R and F. Oliver, 2013. Automated glaucoma detection using hybrid feature extraction in retinal fundus images. J. Mechan. Med. Biol., 13: 1350011-1-1350011-21 DOI: 10.1142/S0219519413500115

Naseri, A., A. Pouyan and N. Kavian, 2012. Automated detection of retinal layers using texture analysis. Int. J. Comput. Applic., 46: 29-33. DOI: 10.5120/6873-8977

Nyul, L.G., 2009. Retinal image analysis for automated glaucoma risk evaluation. Proceedings of the SPIE MIPPR: Medical Imaging, Parallel Processing of Images and Optimization Techniques, Oct.13, IEEE Xplore Press, pp: 1-9. DOI: 10.1117/12.851179

Rajendra, A.U., S. Dua, X. Du, S.V. Sree and C.K. Chua, 2011. Automated diagnosis of glaucoma using texture and higher order spectra features. IEEE Trans. Inf. Technol. Biomed., 15: 449-455. DOI: 10.1109/TITB.2011.2119322

Ramamurthy, B. and K.R. Chandran, 2012. Content based medical image retrieval with texture content using gray level co-occurrence matrix and K-means clustering algorithms. J. Comput. Sci., 8: 1070-1076. DOI: 10.3844/jcssp.2012.1070.1076

Tan, J.H., E.Y.K. Ng., U.R. Acharya and C. Chee, 2010. Study of normal ocular thermo gram using textural parameters. Infrared Phys. Techn., 53: 120-126. DOI: 10.1016/J.INFRARED.2009.10.006

Veluchamy, M., K. Perumal and T. Ponuchamy, 2012. Feature extraction and classification of blood cells using artificial neural network. Am. J. Applied Sci., 9: 615-619. DOI: 10.3844/ajassp.2012.615.619

Yogesh, K.A. and M. Sasikala, 2012. Texture analysis of retinal layers in spectral domain OCT images. Int. J. Emerg. Technol. Adv. Eng., 2: 296-300.